ACS Pharmacology & Translational Science

pubs.acs.org/ptsci

Article

Sustained Release GLP-1 Agonist PT320 Delays Disease Progression in a Mouse Model of Parkinson's Disease

Vicki Wang, Tung-Tai Kuo, Eagle Yi-Kung Huang, Kuo-Hsing Ma, Yu-Ching Chou, Zhao-Yang Fu, Li-Wen Lai, Jin Jung, Hoi-Il Choi, Doo-Sup Choi, Yazhou Li, Lars Olson, Nigel H. Greig, Barry J. Hoffer, and Yuan-Hao Chen*

Cite This: *ACS Pharmacol. Transl. Sci.* 2021, 4, 858–869

Read Online

ACCESS | Metrics & More | Article Recommendations

ABSTRACT: GLP-1 agonists have become increasingly interesting as a new Parkinson's disease (PD) clinical treatment strategy. Additional preclinical studies are important to validate this approach and define the disease stage when they are most effective. We hence characterized the efficacy of PT320, a sustained release formulation of the long acting GLP-1 agonist, exenatide, in a progressive PD (MitoPark) mouse model. A clinically translatable biweekly PT320 dose was administered starting at 5 weeks of age and longitudinally evaluated to 24 weeks, and multiple behavioral/cellular parameters were measured. PT320 significantly improved spontaneous locomotor activity and rearing in MitoPark PD mice. "Motivated" behavior also improved, evaluated by accelerating rotarod performance. Behavioral improvement was correlated with enhanced cellular and molecular indices of dopamine (DA) midbrain function. Fast scan cyclic voltammetry demonstrated protection of striatal and nucleus accumbens DA release and reuptake in PT320 treated MitoPark mice. Positron emission tomography showed protection of striatal DA fibers and tyrosine hydroxylase protein expression was augmented by PT320 administration. Early PT320 treatment may hence provide an important neuroprotective therapeutic strategy in PD.

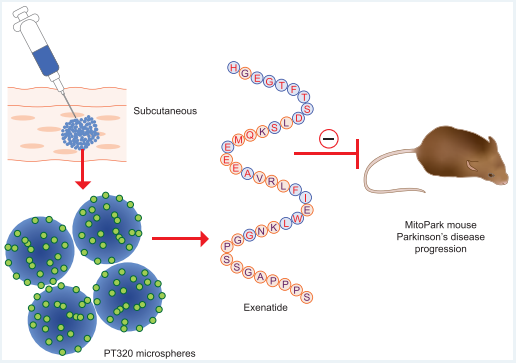

KEYWORDS: *Parkinson's disease, MitoPark mice, exenatide, PT320, GLP-1, exendin-4*

When symptoms of Parkinson's disease (PD) are first apparent, degeneration of the mesencephalic dopamine (DA) circuitry is already severe.[1] However, it is not clear which symptoms are related specifically to degeneration of the ascending dopaminergic pathways, as opposed to changes related to non-dopaminergic systems in other brain areas, the gastrointestinal tract and/or autonomic pathways in the brainstem. In terms of affect and cognitive changes, telencephalic pathways are also potentially involved.

One approach to study the role of progressive degeneration of midbrain DA systems is to target these systems in mice. In our previous work, the mitochondrial transcription factor TFAM was deleted in midbrain DA neurons to generate a PD model termed the MitoPark mouse.[2] In this model, impaired mitochondrial function in DA neurons leads to progressive degeneration of the ascending DA systems. The model permits studies of the role of DA neuron degeneration, studies of DA neuron pathology, and behavioral effects over an extended time of ongoing degenerative events, longer than the degeneration period in most neurotoxin-based PD animal models.[3−5]

Increasing evidence supports glucagon-like peptide-1 receptor (GLP-1R) agonists as a new non-DA PD treatment strategy, mitigating the underlying pathological cascades that drives the disease process. GLP-1-based mimetics are approved for, and effective in, the treatment of type 2 diabetes mellitus (T2DM)[6] with the first agent, exendin-4 (Ex-4, commercially known as exenatide), approved by the US Food and Drug Administration in 2005. Since then, a range of GLP-1R agonists have been developed and approved as treatments for metabolic disorders.[7,8] Whereas the endogenous incretin hormone GLP-1 and longer-acting incretin mimetics that include exenatide (Byetta and Bydureon), liraglutide (Victoza), lixisenatide (Lyxumia), semaglutide (Ozempic), and dulaglutide (Trulicity) are best known for their glucose homeostasis actions and ability to facilitate insulin signaling, they also exert trophic effects, augmenting islet β-cell proliferation and differentiation, inhibiting apoptosis, and improving cellular survival.[6,9] Importantly, they exert multiple extra-pancreatic

Received: January 7, 2021
Published: March 16, 2021

https://dx.doi.org/10.1021/acsptsci.1c00013
ACS Pharmacol. Transl. Sci. 2021, 4, 858–869

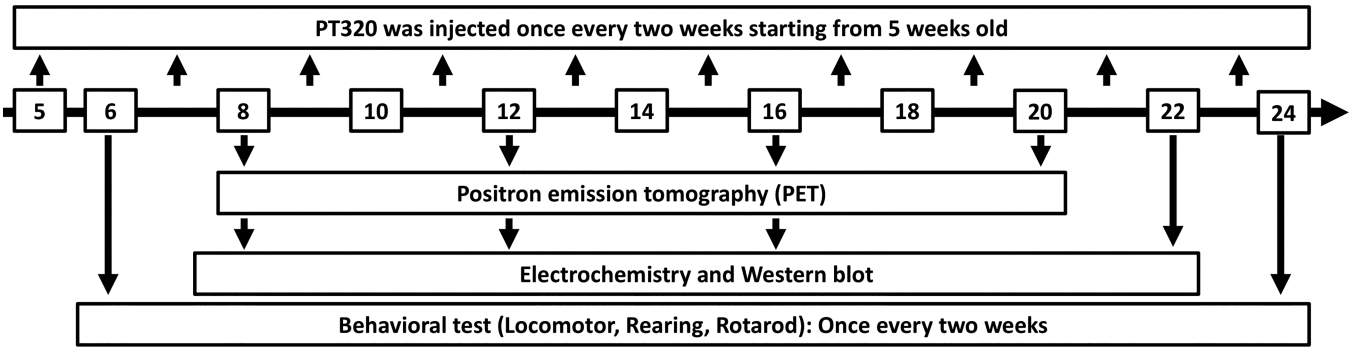

Figure 1. Schematic time line of biweekly administration of PT320 to MitoPark animals and behavioral as well as cellular and molecular tests.

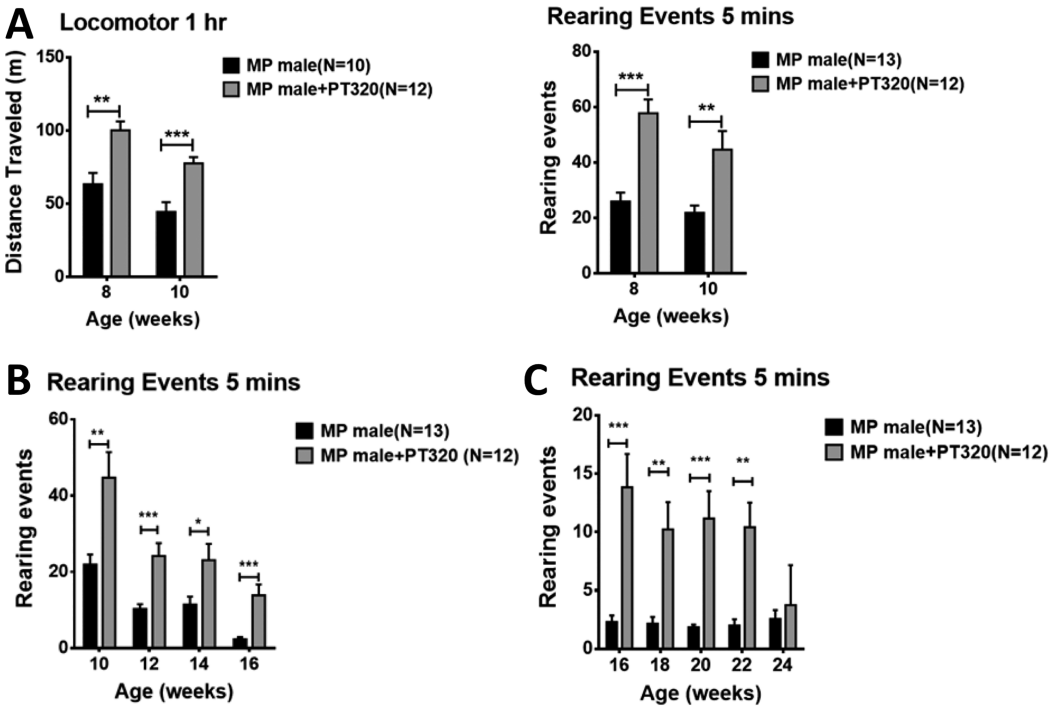

Figure 2. (A) Overall locomotor activity and rearing events in MitoPark mice at early time points (8 and 10 weeks). PT320 administration was initiated at 5 weeks, as this time is in line with the first described changes in mitochondrial morphology.[2] Unpaired *t*-test; **, $p < 0.01$, and ***, $p < 0.001$. (B) Rearing of 10−16 week old MitoPark animals. These time points were selected to coincide with described changes in TH immunocytochemistry and DA levels in striatum, as previously measured with HPLC.[2] Unpaired *t*-test; *, $p < 0.05$; **, $p < 0.01$; and ***, $p < 0.001$. (C) Rearing at later ages (16−24 weeks) of MitoPark mice when there is significant DA loss. Note the changes in ordinate values from those in A and B, since rearing is much impaired at these older ages. Unpaired *t*-test; *, $p < 0.05$; **, $p < 0.01$; and ***, $p < 0.001$.

actions that are independent of glucose homeostasis and mediated via GLP-1Rs expressed on other cell types, including neurons, astrocytes, and microglia. Incretin mimetics including GLP-1 can enter the brain,[10,11] where, if available in a sufficiently high concentration, they can likewise provide trophic, protective, and anti-inflammatory actions. A number of studies have demonstrated neuroprotective and reparative actions, as well as insulin receptor resensitization actions of GLP-1R stimulation across animal models of PD and other neurodegenerative disorders.[7,8,12−15] A recent randomized, double-blind, placebo-controlled trial demonstrated that a GLP-1R agonist improved motor function in moderate PD.[16]

As available GLP-1R agonists were developed for T2DM and metabolic disorders, brain uptake was likely not a factor in initial drug design, but it is clearly an important issue in selecting which of a growing number of agents should best evaluated in human neurodegenerative disorders.[11] Our prior studies demonstrated that subcutaneous administration of exenatide provides brain concentrations that are approximately 2−3% of concomitant plasma levels in humans[16] and in rats,[17] and that these levels are best achieved by steady-state, long-term administration of drug. In this regard, once every 2 week administration of exenatide, in the form of its sustained release formulation PT320 (formerly known as PT302), rapidly achieved steady-state levels in plasma[18−20] and manifested dramatically higher CNS levels than twice daily administration of an immediate release exenatide used clinically as Byetta.[17]

We and others have previously demonstrated that GLP-1R agonists, including exenatide, protect tyrosine hydroxylase immunoreactivity (TH-IR) in primary ventromesenchephalic neuron cultures as well as dopaminergic neuron areas in the brain of rats following 6-hydoxydopamine (6-OHDA) challenge.[21−24] Preservation of DA levels, reduced loss of TH-IR, and improved behavioral function have been noted

https://dx.doi.org/10.1021/acsptsci.1c00013
ACS Pharmacol. Transl. Sci. 2021, 4, 858−869

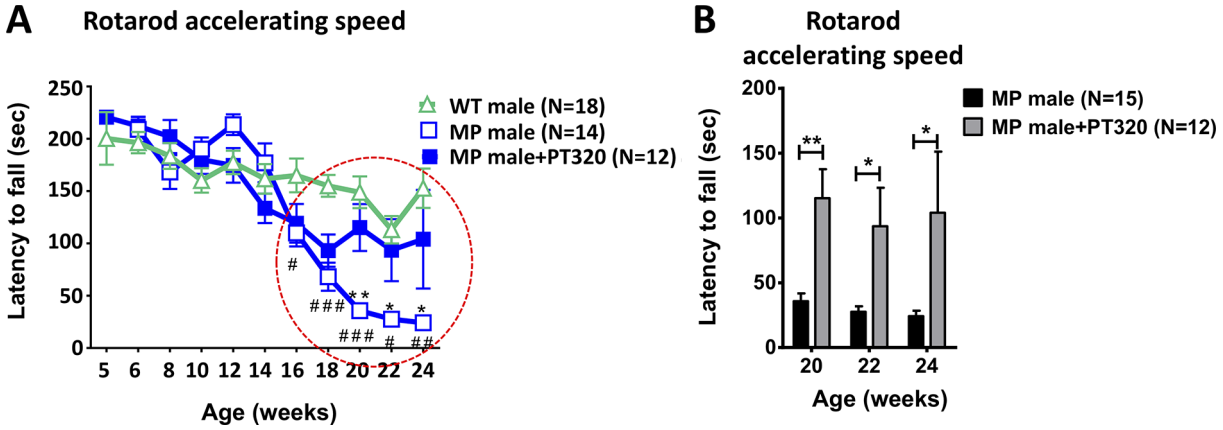

Figure 3. (A) Time course of changes in accelerating rotarod performance at different ages. Note that MitoPark mice treated with PT320 have values almost equal to those of WT animals, whereas untreated MitoPark mice are significantly impaired at later ages (red dashed circle). Two-way analysis of variance (ANOVA) followed by a Bonferroni post hoc test for multiple comparisons. WT male compared to MitoPark (MP) male: $^{\#}$, $p < 0.05$; $^{\#\#}$, $p < 0.01$; and $^{\#\#\#}$, $p < 0.001$. MP male compared to PT320-treated MP male: *, $p < 0.05$; **, $p < 0.01$. (B) Accelerating rotarod performance in 20, 22, and 24 week old MP mice. Unpaired *t*-test: *, $p < 0.05$, and **, $p < 0.01$.

across PD rodent models involving 1-methyl-4phenyl-1,2,3,6 tetrahydropyridine (MPTP) and lipopolysaccharide (LPS) challenge, in addition to 6-OHDA lesioning.[21,25−27]

Neurotoxin-based animal models, although very valuable for drug development, do not perfectly recapitulate the slow progressive onset of PD in humans. The MitoPark mouse is a well characterized PD model that mimics several aspects of the human disorder, including progressive degeneration of DA neurons in substantia nigra and the ventral tegmental area (VTA). Resulting motor deficits can be mitigated by L-DOPA administration.[2,3] The DA circuit degeneration is induced by loss of mitochondrial transcription factor A (TFAM), a protein required for mitochondrial DNA expression and preservation within DA neurons, leaving them respiratory-chain-deficient. Here we characterized the effects of the exenatide sustained-release formulation PT320 in the MitoPark model. We examined drug effects over an extended and previously defined time course in this progressive PD model and demonstrate a substantial mitigation of DA neuron degeneration and PD symptoms over a broad range of measures.

RESULTS

Animals and Exendin-4 Plasma Levels. Behavioral studies were conducted using MitoPark mice either untreated or given PT320. We have previously shown that there are no significant behavioral or neurochemical effects in healthy or 6-OHDA lesioned rodents treated with the PT320 vehicle used here.[22] For fast scan cyclic voltammetry (FSCV), TH, and positron emission tomography (PET) studies, data from wild-type (WT) C57BL/6J mice were included for reference. Male MitoPark mice manifest a PD phenotype earlier and more severely, over the studied 5−24 week time periods, than female MitoPark mice because of the protective effects of estrogen.[28] Thus, only male mice were used in the current study.

Since heterozygote mice were bred to generate the MitoPark animals, equal numbers of both genders are produced. Accordingly, only one of eight offspring yields a male MitoPark mouse as needed for the experiments. In order to ensure an appropriate number of animals for the various behavioral and cellular studies described below, we did not include a third group of MitoPark animals with vehicle alone as noted above. We have previously shown that vehicle injections have no effect on midbrain DA pathways of MitoPark mice.[22]

The time line of biweekly PT320 treatments is shown in Figure 1. The drug proved well-tolerated, as evaluated by animal appearance and weight. Numbers of animals, shown in the figures, were successively reduced at increasing ages since some animals were taken at each age for terminal FSCV and TH measurements. Quantification of plasma Ex-4 levels was undertaken in a parallel group of WT male mice. Samples were obtained at 3, 7, and 14 days following subcutaneous administration of 30 mg PT320/kg, in line with our previous demonstration that a steady state is achieved at 72 h onward.[17,18,22] Averaged across these times, this provided a mean Ex-4 plasma concentration of 2376 ± 447 pg/mL (n = 15), which is in line with both prior rodent studies and clinical relevance.[13,17,22,29]

Behavioral Studies. Motor activity is shown at early (8−10 weeks, Figure 2A), intermediate (10−16 weeks, Figure 2B), and late ages (16−24 weeks, Figure 2C). We focused on rearing in the cylinder test since this depends on axial set, a function of the nigrostriatal DA input. At all ages, PT320-treated animals showed much better horizontal locomotion as well as rearing activity than untreated MitoPark mice. Performance in the accelerating rotarod test depends on motor learning, another well-documented function of the nigrostriatal DA input, as well as motor performance. As shown in Figure 3A and graphically in Figure 3B, older (20−24 weeks) MitoPark mice that had been treated with PT320 were much better at remaining on the rotating rod than untreated MitoPark mice.

Fast Scan Cyclic Voltammetry. Data on DA release in striatum (Figure 4A) and nucleus accumbens (NAc, Figure 4B) are shown in mice studied at 8, 12, 16, and 22 weeks of age. We previously showed that there are only small changes in mitochondrial morphology at 8 weeks and significant changes in the DA nigrostriatal and mesolimbic input at 12−16 weeks in MitoPark mice. At 20−22 weeks of age, there are marked losses of the nigrostriatal DA input evaluated histochemically and biochemically.[2] As in human PD, the mesolimbic DA system is reduced to a lesser extent and more slowly than the nigrostriatal DA system. For the FSCV studies, we used both single pulse (1p) stimulation to mimic tonic DA neuron

https://dx.doi.org/10.1021/acsptsci.1c00013
ACS Pharmacol. Transl. Sci. 2021, 4, 858−869

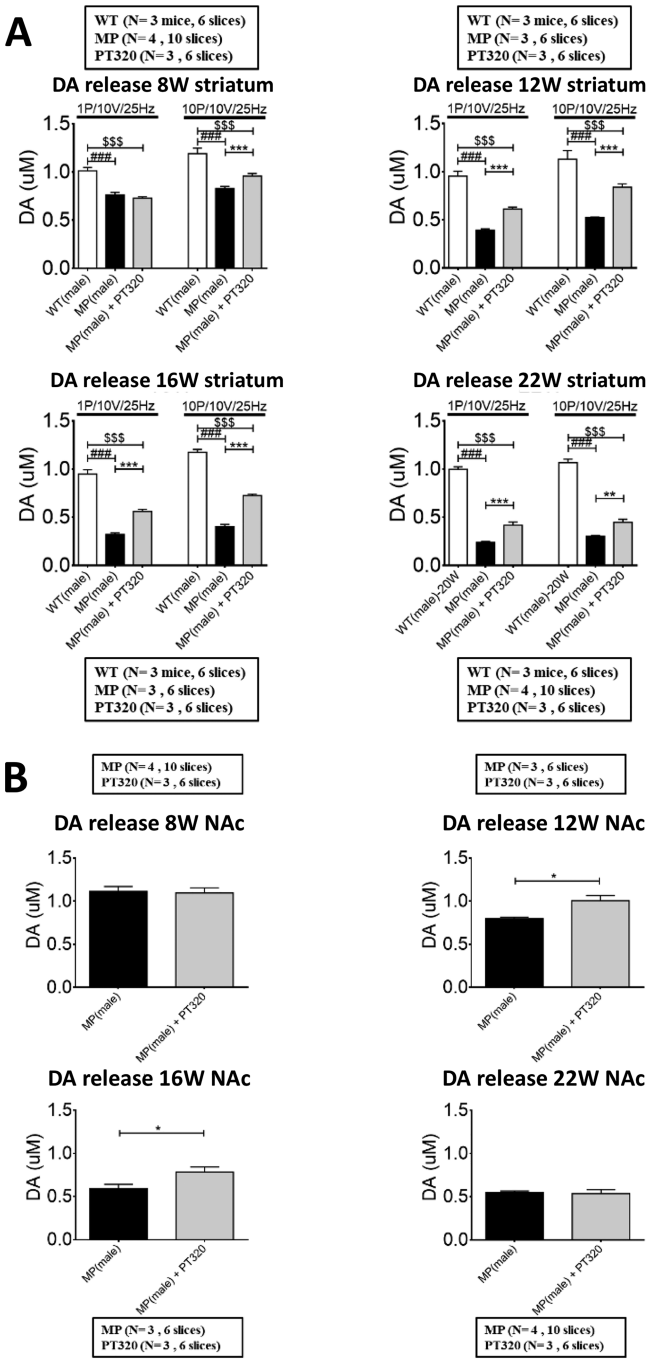

Figure 4. (A) DA release in striatum, studied with FSCV in MitoPark and WT mice at 8 weeks, an age when there is little change in striatal DA, at 12 and 16 weeks, where the changes in DA are significant, and at 22 weeks when changes in behavior and loss of nigrostriatal innervation are still more pronounced. One-way analysis of variance (ANOVA) followed by Bonferroni post hoc test for multiple comparisons. MP vs MP+PT320: ***, $p < 0.001$; WT vs MP: $^{\#\#}$, $p < 0.01$, and $^{\#\#\#}$, $p < 0.001$; WT vs MP+PT320: $^{\$}$, $p < 0.05$, and $^{\$\$\$}$, $p < 0.001$. (B) DA release in nucleus accumbens (NAc) measured by FSCV at 8, 12, 16, and 22 weeks old MitoPark mice. The PT320-induced changes in DA release at 12 and 16 weeks are less than in striatum and are in accord with smaller reductions in the DA input to NAc in MitoPark mice at this age, compared with striatal DA input. One-way analysis of variance (ANOVA) followed by a Bonferroni post hoc test for multiple comparisons. *, $p < 0.05$. Unpaired *t*-test analysis.

activity and phasic (10p) stimulation to mimic DA neuron burst activity. In striatum, DA release was reduced in MitoPark mice compared to WT animals and treatment with PT320 augmented DA release, particularly in 12, 16, and 22-week old MitoPark mice. In the NAc, there was little change at 8 weeks but a significant increase of DA release 12 and 16 weeks old MitoPark mice treated with PT320. There was little difference at 22 weeks of age, perhaps due to fewer GLP-1 receptors in this region.[30,31]

PET Studies. The findings of DA release above, together with the behavioral data presented earlier, suggest PT320 augments DA input to striatum. To further study this, we used PET to label the DA transporter in MitoPark and WT animals. As shown in Figure 5A, although the PET signal was much reduced in both groups of MitoPark mice, the animals treated with PT320 showed significantly larger PET DA transporter signals than untreated MitoPark mice at 12, 16, and 20 weeks of age.

Tyrosine Hydroxylase. TH expression levels in 8, 12, 16, and 22 week old MitoPark mice are shown in Figure 5B. At 8 weeks of age, there was little difference between PT320-treated and untreated MitoPark mice. However, at 12, 16, and 22 weeks of age, when there is significant and progressive loss of striatal DA innervation as previously shown by TH immunocytochemistry,[2,3] TH levels were significantly augmented in the PT320-treated mice as evaluated by Western blots. Indeed, at 12 weeks of age, TH levels in MitoPark animals treated with PT320 were still at WT levels.

DISCUSSION

PD pathophysiology includes both motor and nonmotor deficits, including constipation, implying the involvement of structural and functional changes both in the brain and in peripheral organs.[32,33] However, a major pathology involves degeneration of the ascending DA systems from substantia nigra and the ventral tegmental area to caudate, putamen, and nucleus accumbens and to the cerebral cortex and limbic structures, respectively. As DA neurons degenerate, the remaining DA neurons increase DA synthesis and release, thus partially compensating for the loss of DA circuitry in humans until about 80% of the striatal DA has been lost.[34,35] Similarly, increased TH synthesis in remaining DA fibers after midbrain DA lesions in rodents has been documented.[36−38] The loss of DA neurons in mesencephalon causes loss of DA innervation of cerebral cortex, which may also contribute to cognitive and affective Parkinson symptoms.[39,40]

In MitoPark mice, the lack of the mitochondrial transcription factor TFAM in DA neurons leads to dysfunctional mitochondria, deficient respiratory chain function, and progressive cell death.[2] Since this loss of TFAM is driven by the DAT promoter, all DA neurons that express DAT are affected, including both those projecting to striatal and those projecting to extrastriatal regions. There is also a small loss of DA neurons in the olfactory bulb, whereas tubero-infundibular DA neurons, which do not have DAT, are spared. As a result, the pattern of DA neuron loss in the MitoPark mouse is somewhat similar to that observed and diagnosed in Parkinson patients.

Extensive clinical literature has shown that exercise both delays the onset and reduces the progression of Parkinsonian symptoms.[41] Similarly, exercising MitoPark mice have a delayed onset of motor symptoms compared to sedentary MitoPark mice, and this effect is "dose-dependent".[42] The

https://dx.doi.org/10.1021/acsptsci.1c00013
ACS Pharmacol. Transl. Sci. 2021, 4, 858−869

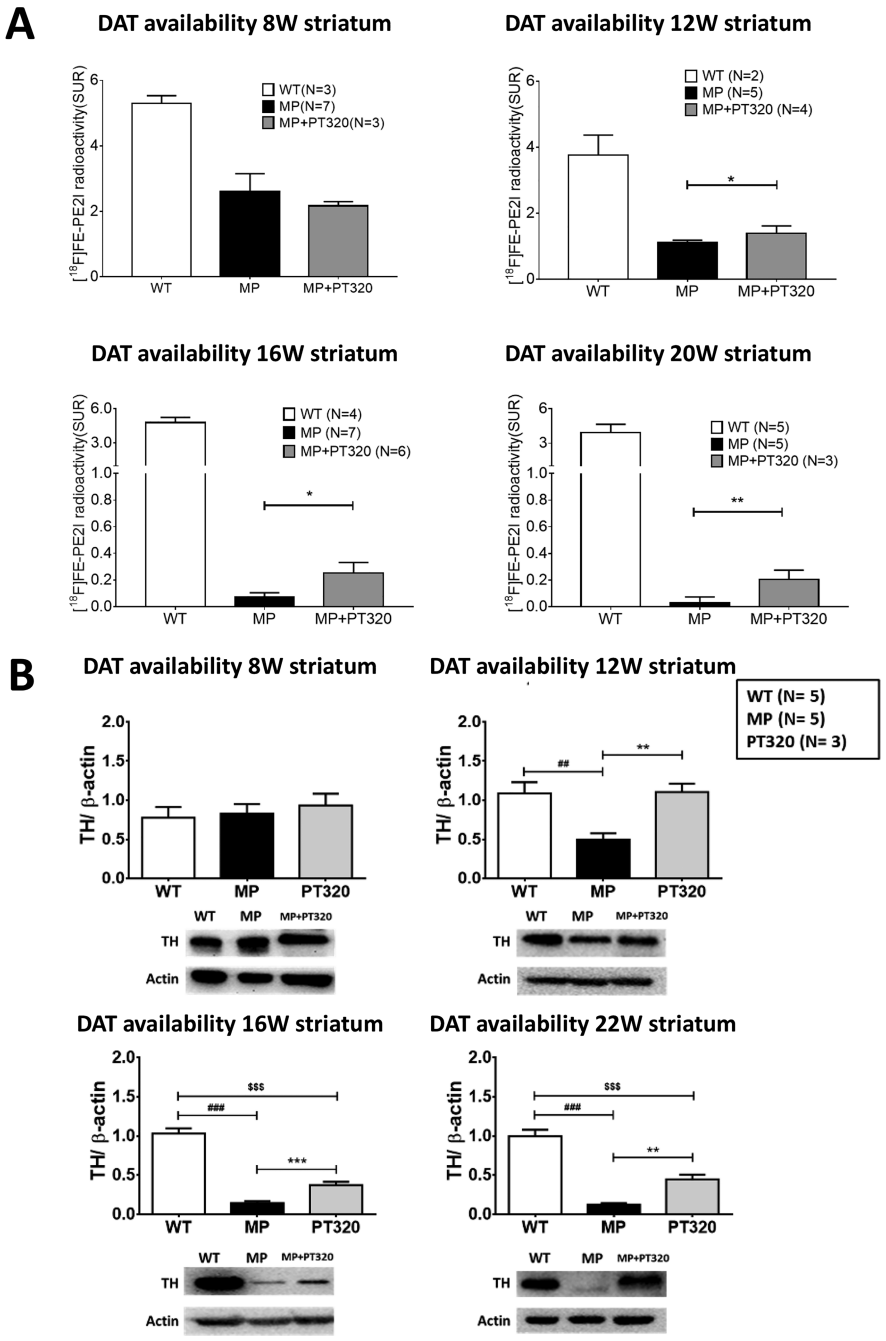

Figure 5. (A) DA Transporter (DAT) expression as a marker of striatal DA fibers in 8, 12, 16, and 20 week old MitoPark animals using PET scans. Although values in the PT320-treated MitoPark mice are less than in WT mice at these ages, they still are significantly greater than the values in untreated MitoPark mice. One-way analysis of variance (ANOVA) followed by a Bonferroni post hoc test for multiple comparisons: *, $p < 0.05$, and **, $p < 0.01$. (B) Changes in TH expression in 8, 12, 16, and 22 week old MitoPark mice. Again, we note little change at 8 weeks but major changes with PT320 in 12, 16, and 22 week old MitoPark mice, as compared to untreated MitoPark animals. Unpaired *t*-test analysis: $^{###}$, $p < 0.001$; *, $p < 0.05$; **, $p < 0.01$; and ***, $p < 0.001$. One-way analysis of variance (ANOVA) followed by Bonferroni post hoc test for multiple comparisons. MP vs MP+PT320: *$p < 0.05$, **$p < 0.01$; ***, $p < 0.001$. WT vs MP: $^{##}$, $p < 0.01$, and $^{###}$, $p < 0.001$. WT vs MP+PT320: $^{$$}$, $p < 0.01$, and $^{$$$}$, $p < 0.001$.

behavioral benefits of exercise in MitoPark mice are accompanied by increased oxidative phosphorylation to generate ATP and elevated striatal DA levels.[42] It is also known that "motivated" behavior is less effected than spontaneous behavior at early and middle stages in PD. This is also evident in MitoPark mice and is associated with correlative changes in DA release and uptake measured with FSCV[43] in striatum and nucleus accumbens. Finally, we note the sex differences in the incidence and progression of PD is well-documented, with males having a higher incidence and more rapid progression.[44] Importantly, we found similar sex differences in MitoPark mice, with male mice having an earlier onset and a more rapid progression of behavioral dysfunction than female mice. This was also associated with more deficits in DA release and reuptake measured by FSCV. After ovariectomy, female MitoPark mice show the same time

https://dx.doi.org/10.1021/acsptsci.1c00013
ACS Pharmacol. Transl. Sci. 2021, 4, 858−869

course of symptoms and deficits of DA presynaptic dynamics as male MitoPark mice, perhaps due to the loss of protective effects of estrogen.[28] Hence, there appears to be multiple parallels between MitoPark mice and human PD progression, supporting the evaluation of treatment strategies that may impact disease progression in the former as a model for the latter. There are several unique properties of the MitoPark model that facilitate this type of study, other than the slow progression of the PD phenotype noted above. First, since this is a genetic model with a strong PD phenotype, there is a uniformity and lack of variability often seen with toxin models. Second, although controversial, there are reports of little or no behavioral changes and DA neuron degeneration, and even some spontaneous recovery, seen with both MPTP and PFF alpha-synuclein toxin models of PD.[45,46] Finally, because the loss of TFAM in MitoPark mice is driven by the DAT promoter, this progressive loss of mitochondrial activity is mostly limited to midbrain DA neurons, versus a more generalized toxicity seen with intracerebral administration.

The major molecular events underlining the neurotrophic, neuroprotective, and anti-inflammatory actions of GLP-1 and, in particular, exenatide, on the nervous system have been characterized in *in vitro* neuronal cultures and in brain. In general, they are analogous to pathways triggered in pancreatic cells related to GLP-1-mediated trophic support and protective actions[7,8,13,15] and appear to be separate from their classical antihyperglycemic actions.[47] Activation of neuronal GLP-1R induces a rapid rise in intracellular cAMP levels and triggers several major signaling pathways. These include the phosphoinositide 3-kinase (PI3K)-AKT pathway, the protein-kinase A (PKA), mitogen-activated protein kinase (MEK), and the extracellular-signal-regulated kinase (ERK/MAPK) pathways with their respective downstream targets, in particular the cyclic AMP response element binding protein (CREB), brain-derived neurotrophic factor (BDNF), and apurinic/apyrimidinic endonuclease 1 (APE1).[48−50] These pathways are known to enhance cellular survival and promote neuroprotection by activating calcium channels, by increasing protein synthesis, mitochondrial biogenesis, DNA repair, and by inhibiting apoptosis and inflammation.[7,8,12,13,48,50−52] Our prior studies of exenatide, in both primary dopaminergic and immortal NSC-19 neuronal cell cultures demonstrated that GLP-1R activation in unchallenged cells enhances their phenotypic robustness by significantly increasing TH and choline acteyltransferase (ChAT) levels, respectively.[21,53] GLP-1R activation also augments cellular survival to physiological and disease-associated insults.[12,14,45,54−56] One of multiple ways that exenatide has been shown to significantly elevate TH levels in neurons is by inducing TH gene expression through the TH promoter,[57] which contains a cAMP-responsive element.[58] This may, in part, underlie the elevation in TH protein described in the current study.

A valuable, albeit complex, feature of the GLP-1 signaling system across cell types is that numerous biochemical cascades associated with neurotrophic, protective, and anti-inflammatory actions are triggered by GLP-1R activation, a specific event induced by GLP-1 agonists. These cascades coalesce by providing pleotropic actions. As a consequence, separating out exclusive pathways that are primarily responsible for individual *in vivo* pharmacological actions is difficult, except by use of selective inhibitors in cellular studies. In relation to mechanisms pertinent to PD, a recent study by Ma and colleagues[59] demonstrated that db/db mice, a classical T2DM preclinical animal model, exhibit a mild (approximately 20%) age-dependent loss of TH-positive staining neurons within substantia nigra. This was significantly mitigated by the incretin mimetic liraglutide and appeared primarily mediated by AMPK/PGC-1α signaling. Prior studies have reported an age-dependent increase in tau phosphorylation in db/db mice,[60] providing a further link to neurodegeneration. Whereas tau pathology is classically associated with Alzheimer's disease and other tau-associated neurodegenerative diseases, recent studies show evidence of tau pathology in PD. A genome-wide association study revealed a close association between tauopathy and sporadic PD,[61] and tau deposition is observed in about 50% of PD brains.[62] Notably, GLP-1R agonists have been found to reduce tau hyperphosphorylation by augmenting Akt activity, which ultimately results in reduced activity of GSK-3β.[63] Moreover, impaired insulin signaling in the brain, which in turn is often associated with PD,[15,64] can inhibit PI3K/Akt and activate GSK-3β, which leads to the enhanced formation of tau-associated neurofibrillary tangles.[65] Such brain insulin resistance is known to be reversed by GLP-1R activation.[15,66] Moreover, neuroinflammation, a common feature of human PD and preclinical rodent models of PD, including MitoPark mice,[67] can be mitigated by GLP-1R agonists.[8,15,68]

Of specific mechanistic relevance to MitoPark mice, it has been reported that GLP-1 and Ex-4 increase mitochondrial mass, mitochondrial membrane potential, and oxygen consumption.[69] In addition, there are several recent reports showing that GLP-1 agonists stimulate mitochondrial biogenesis[70] as well as augment mitochondrial integrity and function.[71] Insofar as the TFAM deletion in MitoPark mice interferes with both mitochondrial biogenesis and function, this literature supports a direct effect of GLP-1 agonists like PT320 on mitochondria as, in part, one potential mechanism for the positive effects seen here.

PT320 is a new SR formulation[19,20] that provides controlled, continuous release of clinical grade Ex-4 following subcutaneous administration. We have studied this compound across mice,[17] rats,[22] nonhuman primates,[18] and humans.[29] There is an initial, controlled, rapid-release Ex-4 burst that provides therapeutic plasma levels within a few hours, by release from the surface of the injected PLGA microspheres. Subsequently, there are slower release phases because of microsphere hydration, creating an *in situ* matrix drug reservoir from which hydrolysis and erosion of the PLGA polymer occurs to liberate embedded drug. This produces a steady-state Ex-4 release and the long-term maintenance of therapeutic drug levels.[72,73] Our prior pharmacokinetic studies of PT320 across animal species have demonstrated both dose-dependent and well-regulated maintenance of plasma Ex-4 levels.[17,18,22,29] Mean plasma values achieved by the PT320 dose, providing 0.6 mg/kg Ex-4 (2% of the 30 mg/kg PT320 dose), in the present study are in line with these prior studies, and indicate that this dose is of clinical relevance.[13]

On the basis of the preclinical efficacy of Ex-4 across animal models of neurodegeneration, and particularly PD, exenatide was evaluated in a single-center, randomized, double-blind, placebo-controlled trial in patients with moderate PD. Motor score improvements in off-medication scores in part 3 of the Movement Disorders Society Unified Parkinson's Disease Rating Scale (MDS-UPDRS) motor subscale were evident following 48 weeks of exenatide and were maintained following drug washout on evaluation at 60 weeks. Following up on this,

https://dx.doi.org/10.1021/acsptsci.1c00013
ACS Pharmacol. Transl. Sci. 2021, 4, 858−869

PT320 is currently in a multicenter Phase 2a clinical trial to evaluate its efficacy and safety in patients with early Parkinson's disease (ClinicalTrials.gov; Identifier: NCT04269642). Our prior studies indicated that Ex-4 provided via subcutaneous PT320 administration resulted in substantially greater brain penetration than the twice daily administration of immediate release Ex-4,[17,22] a formulation initially evaluated in a proof of concept, single-blind trial design in patients with moderate PD.[74]

PT320, given before, or 6 days after unilateral 6-OHDA lesioning, significantly improved TH-IR in the lesioned striatum and substantia nigra pars compacta, and attenuated methamphetamine-induced rotation.[22] However, when given 4 weeks after 6-OHDA lesioning there was little effect on striatal DA levels.[75] These data suggest that early treatment with PT320 can reduce progressive degeneration of existing DA neurons. Hence, PT320 should be given at early stages of human PD, before major loss of DA neurons.

In contrast to most 6-OHDA lesion models, the MitoPark mouse has a slow progressive loss of midbrain DA circuitry. Beginning PT320 treatment at 5 weeks allows a test of PT320 efficacy starting when the DA input is relatively intact.[2] This correlates well with effects of PT320 given before or just after 6-OHDA lesioning and supports the importance of onset time of treatment in that PT320 should be initiated in the early stages of PD in humans, prior to the occurrence of significant DA circuit loss.

METHODS

Animals. The breeding scheme for generating MitoPark mice has been previously described.[2−4] Briefly, mice expressing DA transporter (DAT)-promoter driven Cre recombinase were crossed with floxed Tfam gene expressing mice. Both DAT alleles were maintained using IRES technology. Breeding pairs to generate MitoPark mice were sent to the National Defense Medical Center in Taiwan from a colony maintained at the NIDA (NIH) Intramural Program. MitoPark mice used in these experiments were 5−24 week old males, heterozygous for DAT-cre expression (DAT/DAT^{cre}), and homozygous for the loxP-flanked Tfam gene ($Tfam^{loxP}/Tfam^{loxP}$). Age-matched WT mice were used as controls in PET, TH, and FSCV studies. Male mice were chosen to avoid the confound of estrogen-induced neuroprotection as noted in the Discussion.[28] The heterozygote mating protocol used here produced an average of one MitoPark male per litter, and no animals were used for more than one assay (behavior, biochemistry, imaging) to ensure that any experimental manipulations would not influence our subsequent studies. Thus, to ensure adequate animal numbers for statistical analysis, only three time points (early, mid, and late) were used, rather than tests at all ages 8−22 weeks.

The same brain tissue was used for ex vivo FSCV with both striatal and nucleus accumbens (NAc) brain slices. Genotyping was performed at the Department of Neurological Surgery, Tri-Service General Hospital, National Defense Medical Center, Taipei (NDMC). Animal protocols were approved by the NDMC Animal Care and Use Committee (IACUC 17−156 and IACUC 17−261) and the animal facility at NDMC has full AAALAC accreditation. For times at which behavioral and cellular/molecular tests were performed, as well as times when PT320 was administered; see Figure 1.

On the basis of our previous studies,[17,22] the chosen dose of exenatide in PT320 was 0.6 mg/kg, given subcutaneously once every 2 weeks. As exenatide represents only 2% of the drug available within the formulation of PT320 (the remaining 98% is polymers from which exenatide is slowly released), the total amount of material administered biweekly here was 30 mg/kg of PT320 (equivalent to 0.6 mg/kg of exenatide). As the PT320 microsphere powder does not go into solution, but forms a suspension, the formulation was "vortexed" immediately before each injection, with confirmation that the PT320 material was in suspension prior to administration.

Locomotor Activity. Locomotor activity was evaluated using activity boxes (45 × 45 cm^2) after the animal was habituated in a low-noise experimental environment for 1 h. Backward and forward movements were monitored with a grid of infrared beams over a 1 h period. The horizontal movements were calculated as distance traveled.

Cylinder Test. Rearing postures were assessed using the cylinder test to evaluate vertical movements and axial set. After a 1 h habituation within the low-noise experimental environment, mice were placed in an open-top, clear plastic cylinder (diameter: 20 cm, height 30 cm) for 5 min and behavior was recorded by a video camera. Rearing was measured from the recorded video.

Rotarod Test. To evaluate motor coordination and learning, we used a rotarod test. During a training phase, mice were introduced to walking on the rotating rod (47650 Rota-Rod NG, Ugo Basile, Comerio, Italy) 1 day before being tested. The training was completed when all mice were able to walk forward for 720 s at 15 rpm. The accelerating speed (from 5 to 80 rpm within 240 s) rotarod test was performed 3 times a day every 2 weeks. The time until the animal fell off the rotating rod was recorded by observers blinded to mouse treatment and genotype. Trials were separated by at least 30 min.

[^{18}F]FE-PE2I PET Imaging for Dopamine Transporter Function. Using an automatic synthesizer system (GE TRACERlab FX2 N), radioactive ^{18}F nuclei were produced by a cyclotron. After separation, the tosylethyl-PE2I precursor was dissolved in anhydrous dimethyl sulfoxide, and reacted with $k[^{18}F]$/ Kryptofix2.2.2 at −140° for 5 min, followed by purification using high-performance liquid chromatography with a C18 column, to obtain the PET ligand, [^{18}F]FE-PE2I.[76,77] Separate sets of MitoPark mice aged 8, 12, 16, and 20 weeks were scanned. Tail vein injections of 0.3 mCi [^{18}F]FE-PE2I were performed during anesthesia (5% isoflurane/oxygen mixture for induction, 2% for maintenance). Each injected animal was first kept in a radiation barrier box for 20 min and then transferred to a PET scanner for static image scans with the energy window set from 250 to 700 keV. 3D images of the brain were captured about 20 min after ligand injection. Images were smoothened using a Gaussian algorithm. The specific uptake ratio (SUR) was calculated as SUR = (VOI of striatum) − (VOI of cerebellum)/VOI of cerebellum.[78,79]

Striatal and NAc Brain Slice Preparation. Brain slices were prepared as described previously.[80,81] Following decapitation, brains were removed and immersed in oxygenated ($95\%O_2/5\%CO_2$) cold cutting solution (in mM: sucrose 194, NaCl 30, KCl 4.5, $MgCl_2$ 1, NaH_2PO_4 1.2, glucose 10, and $NaHCO_3$ 26). Coronal 280 μm slices containing striatum and NAc were cut (VT 100, Leica) in a chamber filled with cold cutting solution. The slices were then transferred to a chamber with oxygenated artificial CSF solution (aCSF; in mM: NaCl

https://dx.doi.org/10.1021/acsptsci.1c00013
ACS Pharmacol. Transl. Sci. 2021, 4, 858−869

126, KCl 3, $MgCl_2$ 1.5, $CaCl_2$ 2.4, NaH_2PO_4 1.2, glucose 11, $NaHCO_3$ 26) at 30 °C for 30 min.

Fast Scan Cyclic Voltammetry (FSCV) for Dopamine Measurements in Brain Slices. The protocol for FSCV recording in this study is based on the method we described previously.[82,83] Coronal sections (280 μm) from the MitoPark brains containing striatum and Nac regions at 8, 12, 16, and 22 weeks of age with and without PT320 treatment, recorded in a chamber (0.5 mL, 31−33 °C) filled with aCSF with a perfusion rate of 2 mL/min, were studied. The carbon fibers (7 μm diameter; Goodfellow Corp., Oakdale, PA) were positioned at 100 μm in depth between the separated tips of a bipolar stimulating electrode (FHC Inc., Bowdoin, ME) within striatum or NAc under stereoscopic observation. Pipettes containing the carbon fibers were filled with a solution of 4 M K-acetate/150 mM KCl. The potential of the carbon fiber was driven from −0.4 to 1.0 V and back to −0.4 V using a triangular waveform (400 V/s scan rate, 7 ms duration) applied every 100 ms. A 5 s (50 scan) control period was initially applied to the carbon fiber. We measured voltage stimulation intensity (10 V) instead of current stimulation intensity as used previously.[82] Voltammetric scans, stimulus waveform generation, timing, and data collection were performed using A/D boards (PCI 6052E and PCI-6711E, National Instruments, Austin, TX) and custom LabView-based software (TarHeel CV, courtesy of Drs. Joseph Cheer and Michael Heien, University of North Carolina).

To assess the capacity of axon terminals to release DA during stimulation, 2 types of voltammetric signals were collected at each recording site by using either a single pulse for tonic or 10 pulses delivered at 25 Hz for phasic activity. DA release evoked by a single pulse (tonic release) stimulation represents both the underlying release per pulse and DA uptake by DAT.[84] The level of tonic release depends upon the DA terminal density and the rate of DA uptake by DAT. Phasic stimulation was used to simulate "burst" activity-related release. All the signals were converted to DA concentrations using a calibration performed for each electrode with a 1 μM DA standard solution. All signals used in the analyses matched the expected voltammetric profile for DA.[85]

Western Blots. Mice were euthanized by decapitation, and brains quickly frozen by immersion in liquid nitrogen. Striatal tissue was homogenized in RIPA buffer (TAAR-ZBZ5, Biotools Co., Ltd., Taiwan) with a protease inhibitor cocktail (ab20111, Abcam, Cambridgeshire, United Kingdom). Protein concentration was measured using BCA protein assay kit II (K813, Biovision, Lausen, Switzerland). Subsequently, proteins in tissue lysates were diluted in 2× SDS and denatured at 95 °C for 5 min. Proteins were then electrophoresed on a 12% SDS-polyacrylamide gel and electrotransferred onto a polyvinyl difluoride membrane. After a 45 min incubation with blocking buffer (2% bovine serum albumin with tris-buffered saline with Tween 20 (TBST), membranes were incubated with primary antibodies against TH (1:1000, rabbit, ab75875, Abcam, Cambridge, United Kingdom) and beta-actin (1:5000, rabbit, ab8227, Abcam, Cambridge, United Kingdom) overnight. After washing 3 times with TBST, the membranes were incubated with goat HRP-linked antirabbit IgG antibodies (1:20,000, ab6721, Abcam, Cambridge, United Kingdom) for 1 h, developed with an enhanced chemiluminescence (ECL) detection kit (Amersham Life Sciences, Piscataway, NJ), and imaged with UVP ChemStudio Plus (Analytik Jena AG, Germany). Results were normalized to the levels of beta-actin used as a loading control, and the amount of immunoreactivity was calculated relative to the expression with the corresponding controls.

Pharmacokinetics. Plasma levels of Ex-4 deriving from the subcutaneous administration of 30 mg/kg PT320 (providing 0.6 mg/kg exenatide) were evaluated in a parallel group of male WT mice. Time-dependent blood samples (250 μL) were obtained by lightly lancing the submandibular vein in the cheek area[86] under an approved National Institute on Aging (Baltimore, MD) Animal Care and Use Committee protocol (Protocol No. 331-TGB-2018). Samples were collected at 3, 7, and 14 days following drug administration, when steady-state Ex-4 release from PT320 is known to occur and collected into heparinized tubes maintained on wet ice. These were subsequently centrifuged (10 000 × *g*, 4 min, 4 °C), with the plasma separated and immediately stored at −80 °C. Ex-4 plasma levels were quantified by use of an exenatide fluorescent immunoassay kit (Phoenix Pharmaceuticals Inc., Burlingame, CA), in line with the manufacturer's guidelines. Specifically, an organic solvent extract was achieved by addition of methanol either to the animal study-obtained plasma samples or plasma standards spiked with known amounts of exenatide (20−5000 pg/mL). Quality control standards of 300 pg/mL were also generated. All samples were then assayed in duplicate. Fluorescence was detected with a microplate reader (Tecan GENios Grödig, Austria) at excitation and emission wavelengths of 320 and 420 nm, respectively.

Statistics. FSCV DA release and behavioral tests were analyzed using an unpaired *t*-test or a one or two-way analysis of variance (ANOVA) followed by a Bonferroni post hoc test for multiple comparisons and performed using appropriate software (GraphPad Prism 5.02, GraphPad Scientific, San Diego, CA). A p-value of <0.05 was considered statistically significant.

AUTHOR INFORMATION

Corresponding Author

Yuan-Hao Chen − *Department of Neurological Surgery, Tri-Service General Hospital, National Defense Medical Center, Taipei 11490, Taiwan*; orcid.org/0000-0002-0570-4328; Email: chenyh178@gmail.com

Authors

Vicki Wang − *Graduate Institute of Medical Sciences, National Defense Medical Center, Taipei 11490, Taiwan*

Tung-Tai Kuo − *Graduate Institute of Computer and Communication Engineering, National Taipei University of Technology, Taipei 10608, Taiwan*

Eagle Yi-Kung Huang − *Department of Pharmacology, National Defense Medical Center, Taipei 11490, Taiwan*

Kuo-Hsing Ma − *Graduate Institute of Biology and Anatomy, National Defense Medical Center, Taipei 11490, Taiwan*

Yu-Ching Chou − *National Defense Medical Center School of Public Health, Taipei City 114, Taiwan*

Zhao-Yang Fu − *Department of Neurological Surgery, Tri-Service General Hospital, National Defense Medical Center, Taipei 11490, Taiwan*

Li-Wen Lai − *Graduate Pharmacology, National Defense Medical Center, Taipei 11490, Taiwan*

Jin Jung − *Peptron, Inc., Daejeon 34054, Republic of Korea*

Hoi-Il Choi − *Peptron, Inc., Daejeon 34054, Republic of Korea*

https://dx.doi.org/10.1021/acsptsci.1c00013
ACS Pharmacol. Transl. Sci. 2021, 4, 858−869

Doo-Sup Choi − *Departments of Molecular Pharmacology and Experimental Therapeutics, Mayo Clinic College of Medicine & Science, Rochester, Minnesota 55905-0001, United States;* orcid.org/0000-0002-6796-9938
Yazhou Li − *Drug Design & Development Section, Translational Gerontology Branch, Intramural Research Program, National Institute on Aging, National Institutes of Health, Baltimore, Maryland 21224-6825, United States*
Lars Olson − *Department of Neuroscience, Karolinska Institute, Stockholm 171 77, Sweden*
Nigel H. Greig − *Drug Design & Development Section, Translational Gerontology Branch, Intramural Research Program, National Institute on Aging, National Institutes of Health, Baltimore, Maryland 21224-6825, United States*
Barry J. Hoffer − *Department of Neurosurgery, Case Western Reserve University School of Medicine, Cleveland, Ohio 44106-4915, United States*

Complete contact information is available at: https://pubs.acs.org/10.1021/acsptsci.1c00013

Author Contributions

Y.-H.C.: designed the study, analyzed all the data, and wrote the paper. T.-T.K.: performed and analyzed the FSCV data. V.W. and T.-T.K.: performed and analyzed the FSCV data. V.W. and Z.-Y.F.: performed animal behavior and Western blot studies and analyzed the data. K.-H.M. and L.-W.L.: performed PET studies and analyzed data. E.Y.-K.H. and Y.-C.C.: contributed analytical tools and analyzed data. J.J., H.-I.I.C., and D.S.C.: provided PT320 and vehicle, analyzed compound for purity and in vitro activity, and designed dosage levels. B.J.H. and L.O.: wrote the paper and designed the study. Y.L. and N.G.: performed pharmacokinetic analyses, wrote the paper, and designed the study.

Notes

The authors declare the following competing financial interest(s): J.J. and H.C. are employees of Peptron Inc. D.S.C. is a scientific advisor to Peptron, Inc. The Intramural Research Program of the National Institute on Aging, NIH, and Peptron, Inc., have a Cooperative Research and Development Agreement to develop Ex-4 as a treatment strategy for neurodegenerative disorders for which NIA and Peptron, Inc., hold patent rights via the work of H.C. and N.G. L.O. is a former co-owner of a company owning commercial rights to the MitoPark mouse.

■ ACKNOWLEDGMENTS

Y.C. is supported by The Ministry of Science and Technology of Taiwan, ROC, MOST-2314-B-016-001-MY3 and MOST-108-2314-B-016-027; Medical Research Project grants TSGH-C108-098, TSGH-C108-094, TSGH-D109-100, and TSGH-D109-097 from the Tri-Service General Hospital of Taiwan; the National Defense Medical Center, ROC, MAB-108-025 and grant MND-MAB-110-077. Peptron PT320 research and development is supported by the Technological Innovation R&D Program (S2174574, Republic of Korea); the Bio and Medical Technology Development Program (NRF-2014M3A9B5073868) of the National Research Foundation, Republic of Korea. N.G. and L.Y. are supported by the Intramural Research Program of the National Institute on Aging, National Institutes of Health, USA. B.J.H. is supported by USPHS, NIH, NS0194152-S1. L.O. is supported by the Swedish Research Council (K2012-62X-03185-42-4), and the Swedish Brain Foundation. D.S.C. is supported by the Samuel C. Johnson for Genomics of Addiction Program at Mayo Clinic, and US PHS, NIH AA018779.

■ ABBREVIATIONS

APE1, apurinic/apyrimidinic endonuclease 1; BDNF, brain-derived neurotrophic factor; ChAT, choline acteyltransferase; CREB, cyclic AMP response element binding protein; DA, dopamine; DAT, dopamine transporter; Ex-4, exendin-4; ERK, extracellular-signal-regulated kinase; FSCV, fast scan cyclic voltammetry; GLP-1, glucagon-like peptide-1; GLP-1R, glucagon-like peptide-1 receptor; GSK, glycogen synthase kinase; 6-OHDA, 6-hydoxydopamine; LPS, lipopolysaccharide; MPTP, 1-methyl-4phenyl-1,2,3,6 tetrahydropyridine; TFAM, mitochondrial transcription factor A; MEK, mitogen-activated protein kinase; PD, Parkinson's disease; PI3K, phosphoinositide 3-kinase; PET, positron emission tomography; PKA, protein-kinase A; T2DM, type 2 diabetes mellitus; TH, tyrosine hydroxylase; IR, immunoreactivity; VTA, ventral tegmental area

■ REFERENCES

(1) Braak, H., Ghebremedhin, E., Rüb, U., Bratzke, H., and Del Tredici, K. (2004) Stages in the development of Parkinson's disease-related pathology. *Cell Tissue Res. 318*, 121−134.
(2) Ekstrand, M. I., Terzioglu, M., Galter, D., Zhu, S., Hofstetter, C., Lindqvist, E., Thams, S., Bergstrand, A., Hansson, F. S., Trifunovic, A., et al. (2007) Progressive parkinsonism in mice with respiratory-chain-deficient dopamine neurons. *Proc. Natl. Acad. Sci. U. S. A. 104*, 1325−1330.
(3) Galter, D., Pernold, K., Yoshitake, T., Lindqvist, E., Hoffer, B., Kehr, J., Larsson, N. G., and Olson, L. (2010) MitoPark mice mirror the slow progression of key symptoms and L-DOPA response in Parkinson's disease. *Genes, Brain Behav. 9*, 173−181.
(4) Good, C. H., Hoffman, A. F., Hoffer, B. J., Chefer, V. I., Shippenberg, T. S., Bäckman, C. M., Larsson, N. G., Olson, L., Gellhaar, S., Galter, D., et al. (2011) Impaired nigrostriatal function precedes behavioral deficits in a genetic mitochondrial model of Parkinson's disease. *FASEB J. 25*, 1333−1344.
(5) Sterky, F. H., Lee, S., Wibom, R., Olson, L., and Larsson, N.-G. (2011) Impaired mitochondrial transport and Parkin-independent degeneration of respiratory chain-deficient dopamine neurons in vivo. *Proc. Natl. Acad. Sci. U. S. A. 108*, 12937−12942.
(6) Drucker, D. J. (2018) Mechanisms of action and therapeutic application of glucagon-like peptide-1. *Cell Metab. 27*, 740−756.
(7) Glotfelty, E. J., Delgado, T. E., Tovar-y-Romo, L. B., Luo, Y., Hoffer, B. J., Olson, L., Karlsson, T. E., Mattson, M. P., Harvey, B. K., Tweedie, D., Li, Y., and Greig, N. H. (2019) Incretin Mimetics as Rational Candidates for the Treatment of Traumatic Brain Injury. *ACS Pharmacol. Transl. Sci. 2*, 66−91.
(8) Glotfelty, E. J., Olson, L., Karlsson, T. E., Li, Y., and Greig, N. H. (2020) Glucagon-like peptide-1 (GLP-1)-based receptor agonists as a treatment for Parkinson's disease. *Expert Opin. Invest. Drugs 29*, 595−602.
(9) Müller, T. D., Finan, B., Bloom, S. R., D'Alessio, D., Drucker, D. J., Flatt, P. R., Fritsche, A., Gribble, F., Grill, H. J., Habener, J. F., et al. (2019) Glucagon-like peptide 1 (GLP-1). *Mol. Metab. 30*, 72−130.
(10) Kastin, A. J., and Akerstrom, V. (2003) Entry of exendin-4 into brain is rapid but may be limited at high doses. *Int. J. Obes. 27*, 313−318.
(11) Salameh, T. S., Rhea, E. M., Talbot, K., and Banks, W. A. (2020) Brain uptake pharmacokinetics of incretin receptor agonists showing promise as Alzheimer's and Parkinson's disease therapeutics. *Biochem. Pharmacol. 180*, 114187.
(12) Kim, D. S., Choi, H.-I., Wang, Y., Luo, Y., Hoffer, B. J., and Greig, N. H. (2017) A New Treatment Strategy for Parkinson's

Disease through the Gut−Brain Axis: The Glucagon-Like Peptide-1 Receptor Pathway. *Cell Transplant. 26*, 1560−1571.
(13) Athauda, D., and Foltynie, T. (2018) Protective effects of the GLP-1 mimetic exendin-4 in Parkinson's disease. *Neuropharmacology 136*, 260−270.
(14) Hölscher, C. (2018) Novel dual GLP-1/GIP receptor agonists show neuroprotective effects in Alzheimer's and Parkinson's disease models. *Neuropharmacology 136*, 251−259.
(15) Hölscher, C. (2020) Brain insulin resistance: role in neurodegenerative disease and potential for targeting. *Expert Opin. Invest. Drugs 29*, 333−348.
(16) Athauda, D., Maclagan, K., Skene, S. S., Bajwa-Joseph, M., Letchford, D., Chowdhury, K., Hibbert, S., Budnik, N., Zampedri, L., Dickson, J., Li, Y., Aviles-Olmos, I., Warner, T. T., Limousin, P., Lees, A. J., Greig, N. H., Tebbs, S., and Foltynie, T. (2017) Exenatide once weekly versus placebo in Parkinson's disease: a randomised, double-blind, placebo-controlled trial. *Lancet 390*, 1664−1675.
(17) Bader, M., Li, Y., Lecca, D., Rubovitch, V., Tweedie, D., Glotfelty, E., Rachmany, L., Kim, H. K., Choi, H.-I., Hoffer, B. J., Pick, C. G., Greig, N. H., and Kim, D. S. (2019) Pharmacokinetics and efficacy of PT302, a sustained-release Exenatide formulation, in a murine model of mild traumatic brain injury. *Neurobiol. Dis. 124*, 439−453.
(18) Li, Y., Vaughan, K. L., Tweedie, D., Jung, J., Kim, H. K., Choi, H.-I., Kim, D. S., Mattison, J. A., and Greig, N. H. (2019) Pharmacokinetics of Exenatide in nonhuman primates following its administration in the form of sustained-release PT320 and Bydureon. *Sci. Rep. 9*, 17208.
(19) Peptron, Inc. *SmartDepot Technology*, http://www.peptron.com/ds2_2_1.html (accessed March 7, 2021).
(20) Peptron, Inc. *On-Going Phase II Study of PT320, a Long-Acting Exenatide, the First-In-Class Drug for Parkinson's Disease Therapy*, http://www.peptron.com/ds6_2_1.html (accessed March 7, 2021).
(21) Li, Y., Perry, T., Kindy, M. S., Harvey, B. K., Tweedie, D., Holloway, H. W., Powers, K., Shen, H., Egan, J. M., Sambamurti, K., Brossi, A., Lahiri, D. K., Mattson, M. P., Hoffer, B. J., Wang, Y., and Greig, N. H. (2009) GLP-1 receptor stimulation preserves primary cortical and dopaminergic neurons in cellular and rodent models of stroke and Parkinsonism. *Proc. Natl. Acad. Sci. U. S. A. 106*, 1285.
(22) Chen, S., Yu, S.-J., Li, Y., Lecca, D., Glotfelty, E., Kim, H. K., Choi, H.-I., Hoffer, B. J., Greig, N. H., Kim, D. S., and Wang, Y. (2018) Post-treatment with PT302, a long-acting Exendin-4 sustained release formulation, reduces dopaminergic neurodegeneration in a 6-Hydroxydopamine rat model of Parkinson's disease. *Sci. Rep. 8*, 10722.
(23) Harkavyi, A., Rampersaud, N., and Whitton, P. S. (2013) Neuroprotection by Exendin-4 Is GLP-1 Receptor Specific but DA D3 Receptor Dependent, Causing Altered BrdU Incorporation in Subventricular Zone and Substantia Nigra. *J. Neurodegener. Dis. 2013*, 407152.
(24) Hansen, H. H., Fabricius, K., Barkholt, P., Mikkelsen, J. D., Jelsing, J., Pyke, C., Knudsen, L. B., and Vrang, N. (2016) Characterization of liraglutide, a glucagon-like peptide-1 (GLP-1) receptor agonist, in rat partial and full nigral 6-hydroxydopamine lesion models of Parkinson's disease. *Brain Res. 1646*, 354−365.
(25) Kim, S., Moon, M., and Park, S. (2009) Exendin-4 protects dopaminergic neurons by inhibition of microglial activation and matrix metalloproteinase-3 expression in an animal model of Parkinson's disease. *J. Endocrinol. 202*, 431.
(26) Harkavyi, A., and Whitton, P. S. (2010) Glucagon-like peptide 1 receptor stimulation as a means of neuroprotection. *Br. J. Pharmacol. 159*, 495−501.
(27) Liu, W., Jalewa, J., Sharma, M., Li, G., Li, L., and Hölscher, C. (2015) Neuroprotective effects of lixisenatide and liraglutide in the 1-methyl-4-phenyl-1,2,3,6-tetrahydropyridine mouse model of Parkinson's disease. *Neuroscience 303*, 42−50.
(28) Chen, Y.-H., Wang, V., Huang, E. Y., Chou, Y.-C., Kuo, T.-T., Olson, L., and Hoffer, B. J. (2019) Delayed Dopamine Dysfunction and Motor Deficits in Female Parkinson Model Mice. *Int. J. Mol. Sci. 20*, 6251.
(29) Gu, N., Cho, S.-H., Kim, J., Shin, D., Seol, E., Lee, H., Lim, K. S., Shin, S.-G., Jang, I.-J., and Yu, K.-S. (2014) Pharmacokinetic Properties and Effects of PT302 After Repeated Oral Glucose Loading Tests in a Dose-Escalating Study. *Clin. Ther. 36*, 101−114.
(30) Graham, D. L., Durai, H. H., Trammell, T. S., Noble, B. L., Mortlock, D. P., Galli, A., and Stanwood, G. D. (2020) A novel mouse model of glucagon-like peptide-1 receptor expression: A look at the brain. *J. Comp. Neurol. 528*, 2445−2470.
(31) Cork, S. C., Richards, J. E., Holt, M. K., Gribble, F. M., Reimann, F., and Trapp, S. (2015) Distribution and characterisation of Glucagon-like peptide-1 receptor expressing cells in the mouse brain. *Mol. Metab. 4*, 718−731.
(32) Beitz, J. M. (2014) Parkinson's disease: a review. *Front. Biosci., Scholar Ed. S6*, 65.
(33) Kalia, L. V., and Lang, A. E. (2015) Parkinson's disease. *Lancet 386*, 896−912.
(34) Hornykiewicz, O. (2001) Chemical neuroanatomy of the basal ganglia−normal and in Parkinson's disease. *J. Chem. Neuroanat. 22*, 3−12.
(35) Marsden, C. D. (1990) Parkinson's disease. *Lancet 335*, 948−952.
(36) Wolf, M. E., Zigmond, M. J., and Kapatos, G. (1989) Tyrosine Hydroxylase Content of Residual Striatal Dopamine Nerve Terminals Following 6-Hydroxydopamine Administration: A Flow Cytometric Study. *J. Neurochem. 53*, 879−885.
(37) Salvatore, M. F. (2014) ser31 tyrosine hydroxylase phosphorylation parallels differences in dopamine recovery in nigrostriatal pathway following 6-OHDA lesion. *J. Neurochem. 129*, 548−558.
(38) Yan, H. Q., Ma, X., Chen, X., Li, Y., Shao, L., and Dixon, C. E. (2007) Delayed increase of tyrosine hydroxylase expression in rat nigrostriatal system after traumatic brain injury. *Brain Res. 1134*, 171−179.
(39) Smith, Y., and Villalba, R. (2008) Striatal and extrastriatal dopamine in the basal ganglia: an overview of its anatomical organization in normal and Parkinsonian brains. *Mov. Disord. 23*, S534−547.
(40) Rommelfanger, K. S., and Wichmann, T. (2010) Extrastriatal dopaminergic circuits of the Basal Ganglia. *Front. Neuroanat. 4*, 139.
(41) Mak, M. K. Y., and Wong-Yu, I. S. K. (2019) Exercise for Parkinson's disease. *Int. Rev. Neurobiol. 147*, 1−44.
(42) Lai, J.-H., Chen, K.-Y., Wu, J. C.-C., Olson, L., Brené, S., Huang, C.-Z., Chen, Y.-H., Kang, S.-J., Ma, K.-H., Hoffer, B. J., Hsieh, T.-H., and Chiang, Y.-H. (2019) Voluntary exercise delays progressive deterioration of markers of metabolism and behavior in a mouse model of Parkinson's disease. *Brain Res. 1720*, 146301.
(43) Chen, Y.-H., Hsieh, T.-H., Kuo, T.-T., Kao, J.-H., Ma, K.-H., Huang, E. Y.-K., Chou, Y.-C., Olson, L., and Hoffer, B. J. (2019) Release parameters during progressive degeneration of dopamine neurons in a mouse model reveal earlier impairment of spontaneous than forced behaviors. *J. Neurochem. 150*, 56−73.
(44) Cerri, S., Mus, L., and Blandini, F. (2019) Parkinson's Disease in Women and Men: What's the Difference? *J. Parkinson's Dis. 9*, 501−515.
(45) Henderson, M. X., Sedor, S., McGeary, I., Cornblath, E. J., Peng, C., Riddle, D. M., Li, H. L., Zhang, B., Brown, H. J., Olufemi, M. F., et al. (2020) Glucocerebrosidase Activity Modulates Neuronal Susceptibility to Pathological α-Synuclein Insult. *Neuron 105*, 822−836.e827.
(46) Luk, K. C., Covell, D. J., Kehm, V. M., Zhang, B., Song, I. Y., Byrne, M. D., Pitkin, R. M., Decker, S. C., Trojanowski, J. Q., and Lee, V. M. Y. (2016) Molecular and Biological Compatibility with Host Alpha-Synuclein Influences Fibril Pathogenicity. *Cell Rep. 16*, 3373−3387.
(47) Campbell, J. E., and Drucker, D. J. (2013) Pharmacology, Physiology, and Mechanisms of Incretin Hormone Action. *Cell Metab. 17*, 819−837.

https://dx.doi.org/10.1021/acsptsci.1c00013
ACS Pharmacol. Transl. Sci. 2021, 4, 858−869

(48) Li, Y., Tweedie, D., Mattson, M. P., Holloway, H. W., and Greig, N. H. (2010) Enhancing the GLP-1 receptor signaling pathway leads to proliferation and neuroprotection in human neuroblastoma cells. *J. Neurochem. 113*, 1621−1631.
(49) Ji, C., Xue, G.-F., Lijun, C., Feng, P., Li, D., Li, L., Li, G., and Hölscher, C. (2016) A novel dual GLP-1 and GIP receptor agonist is neuroprotective in the MPTP mouse model of Parkinson′s disease by increasing expression of BNDF. *Brain Res. 1634*, 1−11.
(50) Yang, J.-L., Chen, W.-Y., Chen, Y.-P., Kuo, C.-Y., and Chen, S.-D. (2016) Activation of GLP-1 Receptor Enhances Neuronal Base Excision Repair via PI3K-AKT-Induced Expression of Apurinic/Apyrimidinic Endonuclease 1. *Theranostics 6*, 2015−2027.
(51) Salcedo, I., Tweedie, D., Li, Y., and Greig, N. H. (2012) Neuroprotective and neurotrophic actions of glucagon-like peptide-1: an emerging opportunity to treat neurodegenerative and cerebrovascular disorders. *Br. J. Pharmacol. 166*, 1586−1599.
(52) Athauda, D., and Foltynie, T. (2016) The glucagon-like peptide 1 (GLP) receptor as a therapeutic target in Parkinson's disease: mechanisms of action. *Drug Discovery Today 21*, 802−818.
(53) Li, Y., Chigurupati, S., Holloway, H. W., Mughal, M., Tweedie, D., Bruestle, D. A., Mattson, M. P., Wang, Y., Harvey, B. K., Ray, B., et al. (2012) Exendin-4 ameliorates motor neuron degeneration in cellular and animal models of amyotrophic lateral sclerosis. *PLoS One 7*, e32008.
(54) Perry, T., and Greig, N. H. (2003) The glucagon-like peptides: a double-edged therapeutic sword? *Trends Pharmacol. Sci. 24*, 377−383.
(55) Perry, T., Haughey, N. J., Mattson, M. P., Egan, J. M., and Greig, N. H. (2002) Protection and Reversal of Excitotoxic Neuronal Damage by Glucagon-Like Peptide-1 and Exendin-4. *J. Pharmacol. Exp. Ther. 302*, 881.
(56) Perry, T., Lahiri, D. K., Sambamurti, K., Chen, D., Mattson, M. P., Egan, J. M., and Greig, N. H. (2003) Glucagon-like peptide-1 decreases endogenous amyloid-β peptide (Aβ) levels and protects hippocampal neurons from death induced by Aβ and iron. *J. Neurosci. Res. 72*, 603−612.
(57) Yamamoto, H., Kishi, T., Lee, C. E., Choi, B. J., Fang, H., Hollenberg, A. N., Drucker, D. J., and Elmquist, J. K. (2003) Glucagon-Like Peptide-1-Responsive Catecholamine Neurons in the Area Postrema Link Peripheral Glucagon-Like Peptide-1 with Central Autonomic Control Sites. *J. Neurosci. 23*, 2939.
(58) Lazaroff, M., Patankar, S., Yoon, S. O., and Chikaraishi, D. M. (1995) The Cyclic AMP Response Element Directs Tyrosine Hydroxylase Expression in Catecholaminergic Central and Peripheral Nervous System Cell Lines from Transgenic Mice (*). *J. Biol. Chem. 270*, 21579−21589.
(59) Ma, D., Liu, X., Liu, J., Li, M., Chen, L., Gao, M., Xu, W., and Yang, Y. (2019) Long-term liraglutide ameliorates nigrostriatal impairment via regulating AMPK/PGC-1a signaling in diabetic mice. *Brain Res. 1714*, 126−132.
(60) Kim, B., Backus, C., Oh, S., Hayes, J. M., and Feldman, E. L. (2009) Increased Tau Phosphorylation and Cleavage in Mouse Models of Type 1 and Type 2 Diabetes. *Endocrinology 150*, 5294−5301.
(61) Nalls, M. A., Pankratz, N., Lill, C. M., Do, C. B., Hernandez, D. G., Saad, M., DeStefano, A. L., Kara, E., Bras, J., Sharma, M., et al. (2014) Large-scale meta-analysis of genome-wide association data identifies six new risk loci for Parkinson's disease. *Nat. Genet. 46*, 989−993.
(62) Zhang, X., Gao, F., Wang, D., Li, C., Fu, Y., He, W., and Zhang, J. (2018) Tau Pathology in Parkinson's Disease. *Front. Neurol. 9*, 809.
(63) Ma, D.-L., Chen, F.-Q., Xu, W.-J., Yue, W.-Z., Yuan, G., and Yang, Y. (2015) Early intervention with glucagon-like peptide 1 analog liraglutide prevents tau hyperphosphorylation in diabetic db/db mice. *J. Neurochem. 135*, 301−308.
(64) Fiory, F., Perruolo, G., Cimmino, I., Cabaro, S., Pignalosa, F. C., Miele, C., Beguinot, F., Formisano, P., and Oriente, F. (2019) The Relevance of Insulin Action in the Dopaminergic System. *Front. Neurosci. 13*, 868.
(65) Hurtado, D. E., Molina-Porcel, L., Carroll, J. C., MacDonald, C., Aboagye, A. K., Trojanowski, J. Q., and Lee, V. M. Y. (2012) Selectively Silencing GSK-3 Isoforms Reduces Plaques and Tangles in Mouse Models of Alzheimer's Disease. *J. Neurosci. 32*, 7392.
(66) Talbot, K. (2014) Brain insulin resistance in Alzheimer's disease and its potential treatment with GLP-1 analogs. *Neurodegener. Dis. Manag. 4*, 31−40.
(67) Langley, M., Ghosh, A., Charli, A., Sarkar, S., Ay, M., Luo, J., Zielonka, J., Brenza, T., Bennett, B., Jin, H., Ghaisas, S., Schlichtmann, B., Kim, D., Anantharam, V., Kanthasamy, A., Narasimhan, B., Kalyanaraman, B., and Kanthasamy, A. G. (2017) Mito-Apocynin Prevents Mitochondrial Dysfunction, Microglial Activation, Oxidative Damage, and Progressive Neurodegeneration in MitoPark Transgenic Mice. *Antioxid. Redox Signaling 27*, 1048−1066.
(68) Athauda, D., Gulyani, S., Karnati, H. k., Li, Y., Tweedie, D., Mustapic, M., Chawla, S., Chowdhury, K., Skene, S. S., Greig, N. H., Kapogiannis, D., and Foltynie, T. (2019) Utility of Neuronal-Derived Exosomes to Examine Molecular Mechanisms That Affect Motor Function in Patients With Parkinson Disease: A Secondary Analysis of the Exenatide-PD Trial. *JAMA Neurology 76*, 420−429.
(69) Kang, M. Y., Oh, T. J., and Cho, Y. M. (2015) Glucagon-like peptide-1 increases mitochondrial biogenesis and function in INS-1 rat insulinoma cells. *Endocrinol. Metab. 30*, 216.
(70) Góralska, J., Śliwa, A., Gruca, A., Raźny, U., Chojnacka, M., Polus, A., Solnica, B., and Malczewska-Malec, M. (2017) Glucagon-like peptide-1 receptor agonist stimulates mitochondrial bioenergetics in human adipocytes. *Acta Biochim. Polym. 64*, 423−429.
(71) Timper, K., del Río-Martín, A., Cremer, A. L., Bremser, S., Alber, J., Giavalisco, P., Varela, L., Heilinger, C., Nolte, H., Trifunovic, A., et al. (2020) GLP-1 Receptor Signaling in Astrocytes Regulates Fatty Acid Oxidation, Mitochondrial Integrity, and Function. *Cell Metab. 31*, 1189−1205.e13.
(72) Wan, F., and Yang, M. (2016) Design of PLGA-based depot delivery systems for biopharmaceuticals prepared by spray drying. *Int. J. Pharm. 498*, 82−95.
(73) Schwendeman, S. P., Shah, R. B., Bailey, B. A., and Schwendeman, A. S. (2014) Injectable controlled release depots for large molecules. *J. Controlled Release 190*, 240−253.
(74) Aviles-Olmos, I., Dickson, J., Kefalopoulou, Z., Djamshidian, A., Ell, P., Soderlund, T., Whitton, P., Wyse, R., Isaacs, T., Lees, A., Limousin, P., and Foltynie, T. (2013) Exenatide and the treatment of patients with Parkinson's disease. *J. Clin. Invest. 123*, 2730−2736.
(75) Yu, S.-J., Chen, S., Yang, Y.-Y., Glotfelty, E. J., Jung, J., Kim, H. K., Choi, H.-I., Choi, D.-S., Hoffer, B. J., Greig, N. H., and Wang, Y. (2020) PT320, Sustained-Release Exendin-4, Mitigates L-DOPA-Induced Dyskinesia in a Rat 6-Hydroxydopamine Model of Parkinson's Disease. *Front. Neurosci. 14*, 785.
(76) Stepanov, V., Krasikova, R., Raus, L., Loog, O., Hiltunen, J., and Halldin, C. (2012) An efficient one-step radiosynthesis of [18F] FE-PE2I, a PET radioligand for imaging of dopamine transporters. *J. Labelled Compd. Radiopharm. 55*, 206−210.
(77) Bang, J.-I., Jung, I. S., Song, Y. S., Park, H. S., Moon, B. S., Lee, B. C., and Kim, S. E. (2016) PET imaging of dopamine transporters with [18F] FE-PE2I: Effects of anti-Parkinsonian drugs. *Nucl. Med. Biol. 43*, 158−164.
(78) Ma, K.-H., Huang, W.-S., Kuo, Y.-Y., Peng, C.-J., Liou, N.-H., Liu, R.-S., Hwang, J.-J., Liu, J.-C., Chen, H.-J., and Shiue, C.-Y. (2009) Validation of 4-[18F]-ADAM as a SERT imaging agent using micro-PET and autoradiography. *NeuroImage 45*, 687−693.
(79) Li, I. H., Huang, W.-S., Shiue, C.-Y., Huang, Y.-Y., Liu, R.-S., Chyueh, S.-C., Hu, S.-H., Liao, M.-H., Shen, L.-H., Liu, J.-C., et al. (2010) Study on the neuroprotective effect of fluoxetine against MDMA-induced neurotoxicity on the serotonin transporter in rat brain using micro-PET. *NeuroImage 49*, 1259−1270.
(80) Chen, Y. H., Harvey, B. K., Hoffman, A. F., Wang, Y., Chiang, Y. H., and Lupica, C. R. (2008) MPTP-induced deficits in striatal synaptic plasticity are prevented by glial cell line-derived neurotrophic factor expressed via an adeno-associated viral vector. *FASEB J. 22*, 261−275.

https://dx.doi.org/10.1021/acsptsci.1c00013
ACS Pharmacol. Transl. Sci. 2021, 4, 858−869

(81) Good, C. H., Wang, H., Chen, Y. H., Mejias-Aponte, C. A., Hoffman, A. F., and Lupica, C. R. (2013) Dopamine D4 receptor excitation of lateral habenula neurons via multiple cellular mechanisms. *J. Neurosci. 33*, 16853−16864.
(82) Chen, Y.-H., Huang, E. Y.-K., Kuo, T.-T., Hoffer, B. J., Miller, J., Chou, Y.-C., and Chiang, Y.-H. (2017) Dopamine release in the nucleus accumbens is altered following traumatic brain injury. *Neuroscience 348*, 180−190.
(83) Cho, H.-Y., Reddy, S. P., and Kleeberger, S. R. (2006) Nrf2 Defends the Lung from Oxidative Stress. *Antioxid. Redox Signaling 8*, 76−87.
(84) Wightman, R. M., and Zimmerman, J. B. (1990) Control of dopamine extracellular concentration in rat striatum by impulse flow and uptake. *Brain Res. Rev. 15*, 135−144.
(85) Kawagoe, K. T., Zimmerman, J. B., and Wightman, R. M. (1993) Principles of voltammetry and microelectrode surface states. *J. Neurosci. Methods 48*, 225−240.
(86) Golde, W. T., Gollobin, P., and Rodriguez, L. L. (2005) A rapid, simple, and humane method for submandibular bleeding of mice using a lancet. *Lab Animal 34*, 39−43.

https://dx.doi.org/10.1021/acsptsci.1c00013
ACS Pharmacol. Transl. Sci. 2021, 4, 858−869